Even-odd Xe and Ba isotopes in the interacting boson-fermion model

H. C. Chiang and S. T. Hsieh
Department of Physics, National Tsing Hua University, Hsinchu, Taiwan 30043, Republic of China

D. S. Chuu
Department of Electrophysics, National Chiao Tung University, Hsinchu, Taiwan, Republic of China
(Received 2 December 1988)

The even-odd Xe and Ba isotopes were studied in the averaged multi-j fermion orbit interacting boson-fermion model I. The agreements of the experimental and calculated energy spectra are quite good. The analyses on wave functions indicate that the mixture of fermion orbits increases and the quasiband structure becomes less prominent for the heavier even-odd Xe and Ba isotopes. The $B(E2)$ values for ^{131,133}Xe were calculated and compared with the experimental data.

I. INTRODUCTION

In recent years, considerable experimental information of the transitional nuclei with $Z > 50$ became available. For example, quite abundant experimental data on the even-odd Xe and Ba isotopes had been collected in the past decade. Theoretical collective models of various versions were used to correlate the data. Both the triaxial-rotor core and vibrational-core plus particle models were applied with reasonable success.[1-6] Either type of the core-particle model could correlate the experimental data of a definite parity. The interacting boson-fermion model, which does not distinguish the neutron and proton bosons (denoted as IBFA-1 hereafter) was applied to analyze the data for both parities.[7-9] The model was extended to include the neutron and proton degrees of freedom (denoted as IBFA-2 hereafter). The IBFA-2 model was applied successfully to the analyses of the Cs and Xe isotopes.[10] This version of the model has the advantage of being closer to the microscopic models. However, since the sizes of the model space are usually large, some truncation method like the weak coupling scheme has to be introduced. In many cases, several fermion single-particle orbits have to be included in the calculation. In order to reduce the number of the boson-fermion interaction parameters, BCS-type (Bardeen-Cooper-Schrieffer) calculations were used to correlate the interaction parameters corresponding to different fermion single-particle orbits.[11] This method was used in both IBFA-1 and IBFA-2 models. It was pointed out by Iachello and Talmi that such an approach overemphasized the pairing interaction and treated the $L=0$ pair and $L=2$ pair in very different ways.[12] This means that the BCS-type correlations to the interaction parameters may be too restrictive. On the other hand, it was found that a multi-j orbit calculation with BCS correlations could be replaced by a single-j orbit calculation by a "renormalization" of the single-j orbit boson-fermion interaction parameters.[13] This, in turn, suggests that the effects of occupation-number-distribution correlations in the interactions may be absorbed in the renormalizations of the interaction parameters. This approach has the advantage of simplicity and can avoid the artificial BCS type of restrictions of the boson-fermion interactions. In this work, we use the BCS method to compute all single quasiparticle energies but relax its restrictions imposed on the boson-fermion interactions. The model is applied to the positive parity states of the even-odd Xe and Ba isotopes. In Sec. II, the details of the model will be described. In Sec. III, the results on energy levels and electromagnetic transition rates will be presented. Finally, the summaries and conclusions will be presented.

II. THE MODEL

In the calculation, the model space will be spanned by the basis states $|n_s n_d v \alpha L, j\rangle_{JM}$ which is given by the coupling of the boson states $|n_s n_d v \alpha L\rangle$ and the single-particle fermion states. In this work, we consider only the positive parity states of the Xe and Ba isotopes. Therefore, the available j orbits in the nearest major shell are the $3s_{1/2}$, $2d_{3/2}$, $2d_{5/2}$, and $1g_{7/2}$ orbits. In the boson core the IBA-1 basis states are used. It was shown that the difference between IBA-1 and IBA-2 were less prominent in the transitional regions far from the closed shells.[14]

The Hamiltonian adopted is of the following form:

$$H = H_B + H_F + H_{\rm BF} \ .$$

Here H_B is the Hamiltonian of IBA-1, i.e.,

$$H_B = n_d \epsilon_d + a_0 p^\dagger \cdot p + a_1 L \cdot L + a_2 Q \cdot Q \ ,$$

where the less important octupole and hexadecapole terms are omitted. The fermion Hamiltonian contains only the one-body terms,

$$H_F = \sum_{jm} E_j a^\dagger_{jm} a_{jm} \ ,$$

where E_j is the quasiparticle energy.

The boson-fermion Hamiltonian contains the quadrupole-quadrupole and the exchange force terms

$$H_{\mathrm{BF}}=kQ_B\cdot Q_F+\sum_{j,\tilde{j},k}\Lambda^k_{j\tilde{j}}:[(a^\dagger_j\times\tilde{d})^{(k)}\times(d^\dagger\times\tilde{a}_{\tilde{j}})^{(k)}]^{(0)}:\ ,$$

where Q_B is the boson quadrupole operator

$$Q_B=(s^\dagger\times\tilde{d}+d^\dagger\times\tilde{s})^{(2)}+\chi(d^\dagger\times\tilde{d})^{(2)}$$

and the SU(3) value of $\chi=-\sqrt{7}/2$ is adopted in this work. Q_F is the fermion quadrupole operator,

$$Q_F=\sum_{j_1,j_2}q_{j_1j_2}(a^\dagger_{j_1}\times\tilde{a}_{j_2})^{(2)}$$

with

$$q_{j_1j_2}=\frac{1}{\sqrt{5}}\langle j_1||Y^{(2)}||j_2\rangle\ .$$

The second term in H_{BF} is the exchange force term and the :: symbol means normal ordering of the operators in between, and

$$\Lambda^k_{j\tilde{j}}=-2\Lambda[(2k+1)/5]^{-1/2}\langle j||Y^2||k\rangle\langle k||Y^2||\tilde{j}\rangle\ .$$

Note all occupation-number-distribution correlations in H_{BF} adopted in the standard IBFA models are omitted. The summation in the exchange force term runs over all fermion single-particle orbitals.

The monopole-monopole term which is adopted in the other similar calculations is omitted in this work. This term is proportional to n_d and can be absorbed in the $n_d\epsilon_d$ term in H_B by a renormalization of ϵ_d.

The fermion quasiparticle energies were determined from the gap equations

$$E_j=[(\epsilon_j-\lambda)^2+\Delta^2]^{1/2}\ ,$$

$$v_j^2=\tfrac{1}{2}[1-(\epsilon_j-\lambda)/E_j]\ ,$$

subject to the constraint of conservation of the number of valence nucleons

$$n=\sum_j v_j^2(2j+1)\ .$$

The unperturbed single-particle energies ϵ_j are extracted from the experimental energy spectrum of ^{131}Sn.[15] Using the gap energy $\Delta=12A^{-1/2}$ MeV as usual,[16] and with the input of unperturbed single-particle energies the gap equation can be solved to get the fermion quasiparticle energies E_j. The quasiparticle energies used in this work are summarized in Figs. 1 and 2.

The boson interaction parameters were determined from a least-squares calculation on the energy spectra of the boson-core nuclei. The adopted boson interaction parameters are summarized in Table I. In the calculations with the even-odd isotopes, it was found that the features of the energy spectra remained essentially the same when ϵ_d were renormalized. This, in turn, suggests that the monopole-monopole term is not important and the value of ϵ_d corresponding to the core nuclei calculation was adopted in the calculation with even-odd nuclei. This left us with only two free varying boson-fermion interaction parameters, κ and Λ in the model. The two parameters were determined by least-squares calculations on the energy spectra of the even-odd Xe and Ba isotopes. If a set

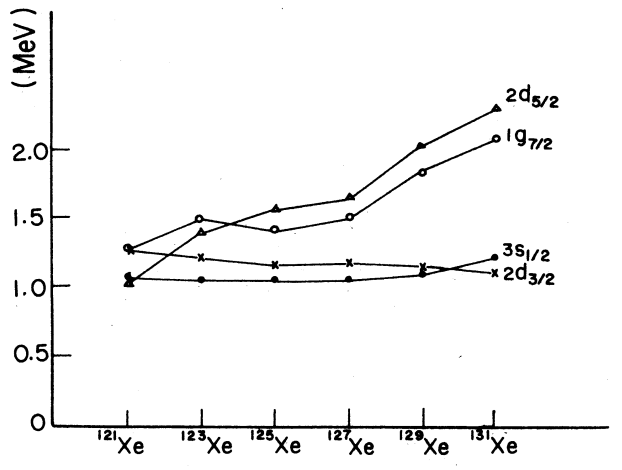

FIG. 1. The fermion quasiparticle energies for the Xe isotopes adopted in this work.

of j-independent κ and Λ parameters can be found to produce good results, it will suggest the justification of the relaxation of the BCS correlations of the boson-fermion interactions. The boson-fermion interaction parameters adopted in this work are summarized in Table II. Note the magnitudes of the parameters are smaller than those used in Ref. 9 since the factors of the occupation number distributions are omitted in this work. Therefore, the overall interaction strengths adopted in this work are rather difficult to compare with those used in Ref. 9. It was found that the obtained parameters vary smoothly versus the change of the mass numbers in each isotope string. The calculated wave functions can be used to calculate the $B(E2)$ values of the electromagnetic transitions. This serves as a further test of the model.

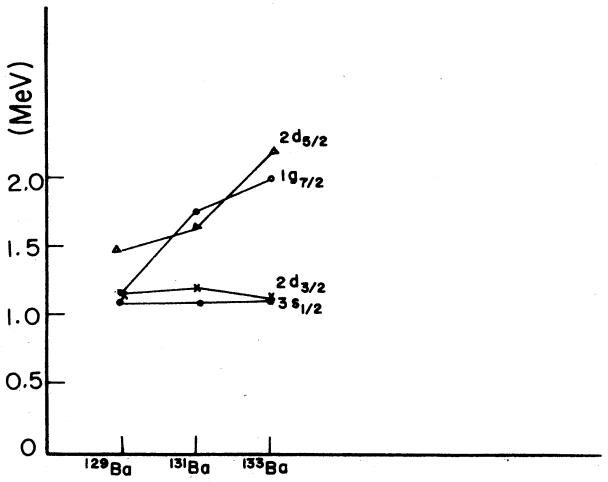

FIG. 2. The fermion quasiparticle energies for the Ba isotopes adopted in this work.

TABLE I. Boson-boson interaction parameters in MeV.

	^{122}Xe	^{124}Xe	^{126}Xe	^{128}Xe	^{130}Xe	^{132}Xe	^{130}Ba	^{132}Ba	^{134}Ba
ϵ_d	0.620	0.620	0.640	0.690	0.780	0.860	0.660	0.680	0.760
a_0	0.090	0.100	0.110	0.150	0.200	0.200	0.130	0.120	0.175
a_1	0.0090	0.0090	0.0090	0.0080	0.0055	0.0030	0.0080	0.0095	0.0130
a_2	−0.0010	−0.0010	−0.0010	−0.0010	−0.0010	0.0050	−0.0040	−0.0005	0.0010

TABLE II. Boson-fermion interaction parameters in MeV.

	^{121}Xe	^{123}Xe	^{125}Xe	^{127}Xe	^{129}Xe	^{131}Xe	^{129}Ba	^{131}Ba	^{133}Ba
K	−0.022	−0.038	−0.038	−0.038	−0.054	−0.083	−0.018	−0.020	−0.050
Λ	0.088	0.076	0.070	−0.011	−0.280	−0.290	0.200	−0.250	−0.320

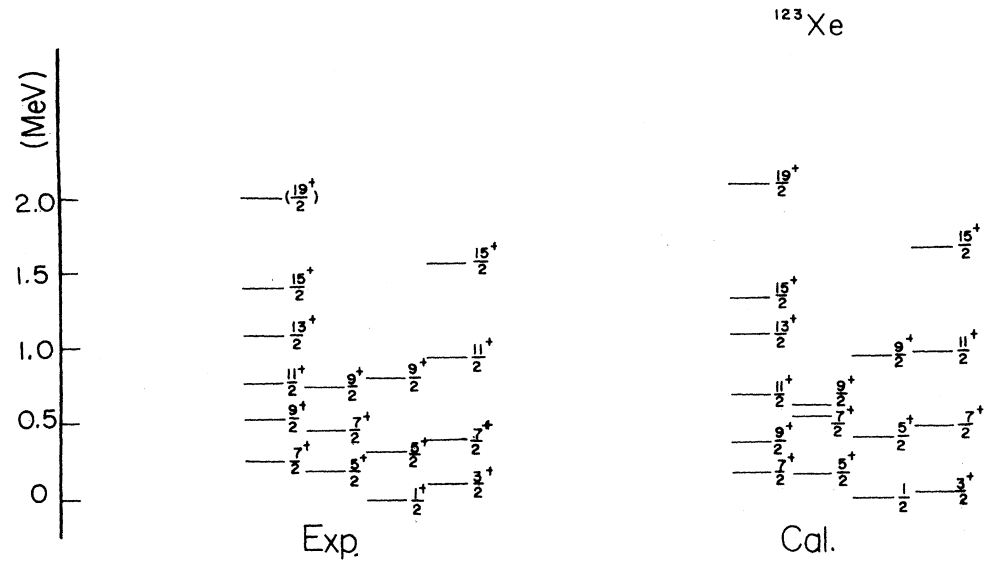

FIG. 3. The calculated and experimental energy spectra for ^{123}Xe. The experimental data are adopted from Ref. 21.

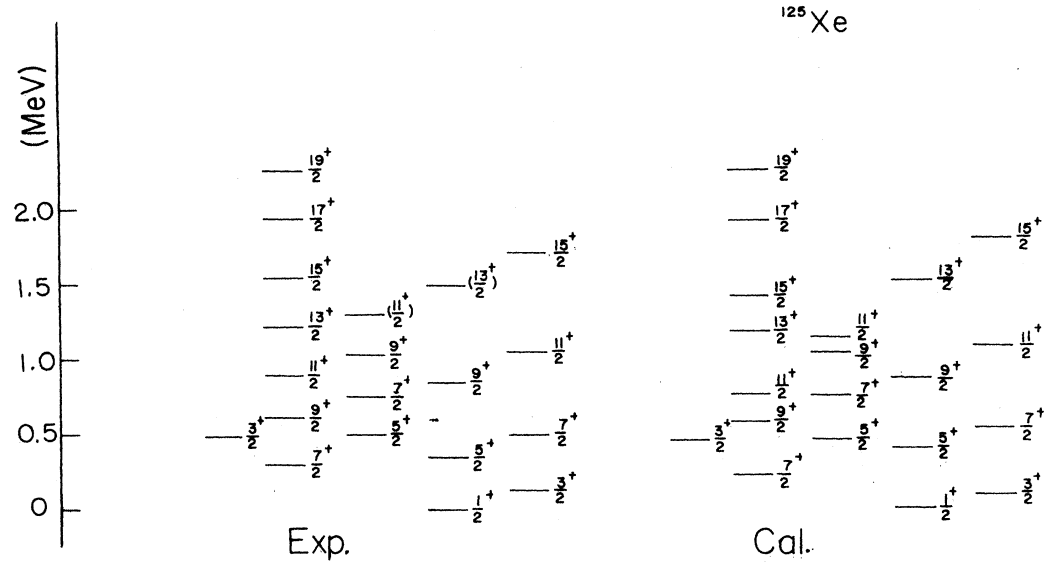

FIG. 4. The calculated and experimental energy spectra for ^{125}Xe. The experimental data are adopted from Ref. 22.

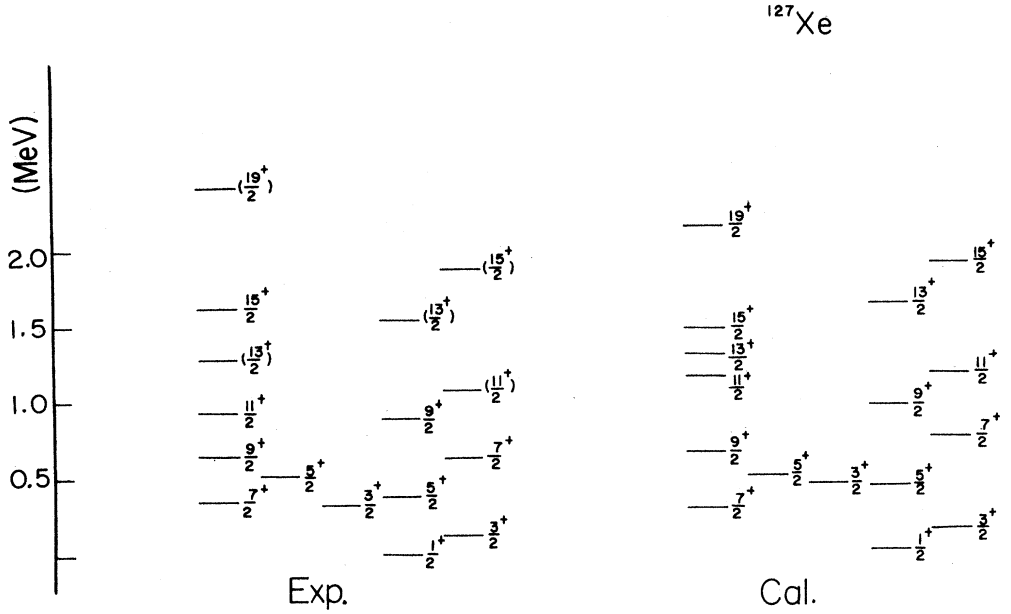

FIG. 5. The calculated and experimental energy spectra for ^{127}Xe. The experimental data are adopted from Ref. 23.

III. RESULTS

A. Energy spectra

(i) Xe isotopes. For the Xe isotopes we select the energy spectra of the $^{123-129}$Xe isotopes for illustrations since more abundant experimental data are available. The experimental and calculated energy spectra are shown in Figs. 3–6. The energy spectra are displayed in different quasibands. In each quasiband, states are related with relatively stronger observed intensities of electromagnetic transitions, although cross-band transitions are not strictly forbidden. In the calculations, all states are calculated relative to the ground states. In other words, no constraints were applied to make the calculated bandheads agree with the experimental values. This has the advantage of checking whether the positions of the bandheads

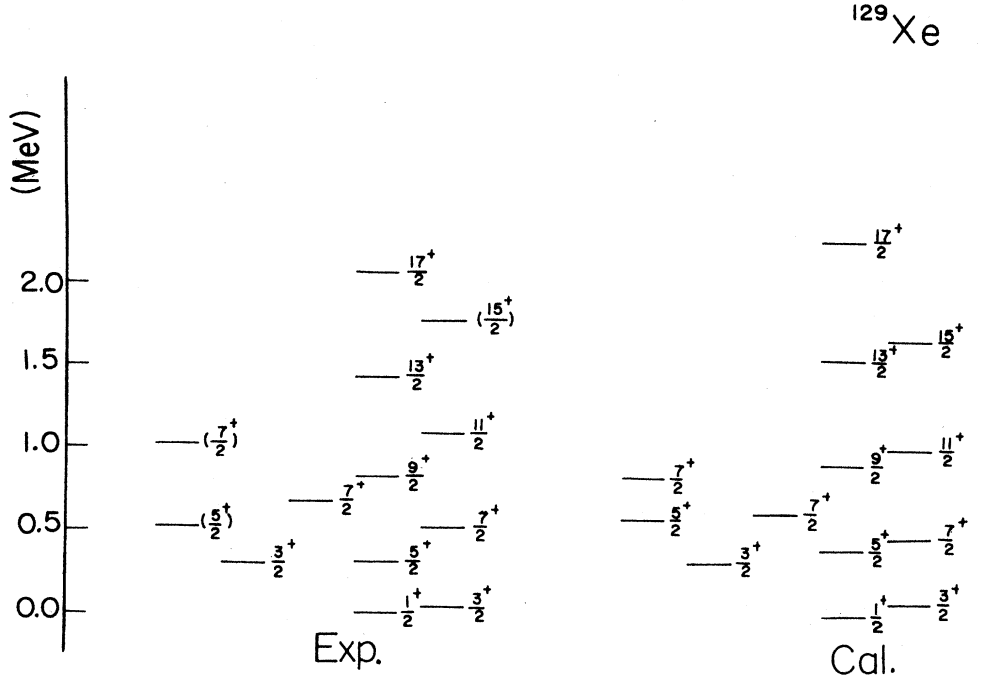

FIG. 6. The calculated and experimental energy spectra for ^{129}Xe. The experimental data are adopted from Ref. 23.

can be produced approximately. From the figures, we see that the calculated energy spectra agree with the experimental data quite well in general. The energy spectra of ^{123,125}Xe are characterized by four quasibands. They include a $(\frac{7}{2})^+$ band, a $(\frac{5}{2})^+$ band with $\Delta I=1$, a $(\frac{1}{2})^+$ band, and a $(\frac{3}{2})^+$ band with $\Delta I=2$. Going to ^{127}Xe the $(\frac{5}{2})^+$ quasiband disappears and both $(\frac{5}{2})^+$ and $(\frac{7}{2})^+$ bands disappear for ^{129}Xe. These results are consistent with the trend in the quasifermion energies. From Fig. 1 we see that $E_{1/2}$ and $E_{3/2}$ do not change much versus the change in neutron number while $E_{5/2}$ is already quite high for ^{127}Xe. Also, from ^{127}Xe to ^{129}Xe, $E_{7/2}$ increases quite rapidly. Therefore, it is difficult to form a band in the low excitation energy regions based on such high quasiparticle energies.

(ii) Barium isotopes. The calculated and experimental energy spectra for $^{129-133}$Ba are shown in Figs. 7–9. Again, the agreement between the calculated and experimental energy spectra is quite satisfactory in general. Owing to the uncertainties in the experimental data, it is impossible to divide the energy spectra into one or more quasibands. Generally speaking, the low-lying states are strongly mixed, and we do not expect clear quasibands built on the single quasiparticle states. In fact, in our calculation only the $(\frac{7}{2})_1^+$, $(\frac{9}{2})_1^+$, $(\frac{11}{2})_1^+$, $(\frac{13}{2})_1^+$, and $(\frac{15}{2})_1^+$ states of ^{129}Ba have quite pure $1g_{7/2}$ configurations and seem to form a band. For other states, there is not enough information to make any band assignment.

B. Wave functions

The wave function intensities corresponding to different fermion single-particle orbits for ^{123}Xe are summarized in Table III. There are several tendencies that can be detected from the table. In general, the lowest $(\frac{1}{2})^+$, $(\frac{3}{2})^+$, $(\frac{5}{2})^+$, $(\frac{7}{2})^+$ states are single-particle states. Therefore, their wave functions are usually dominated by the corresponding fermion single-particle orbit configurations. In general, the wave functions for the other Xe isotopes show similar features but with the tendency that the dispersion of configurations increases as

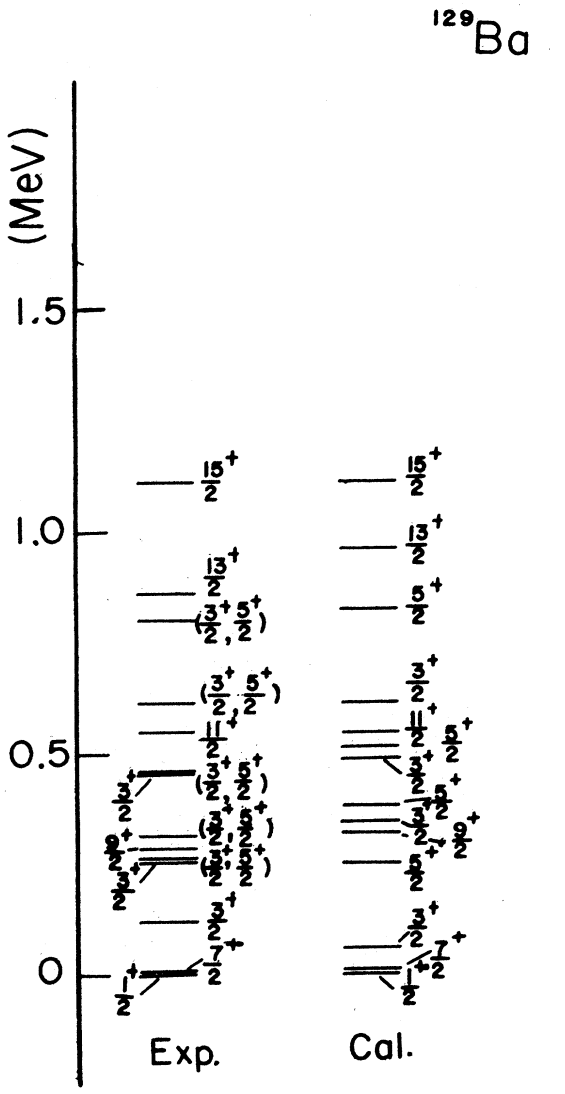

FIG. 7. The calculated and experimental energy spectra for ^{129}Ba. The experimental data are adopted from Ref. 24.

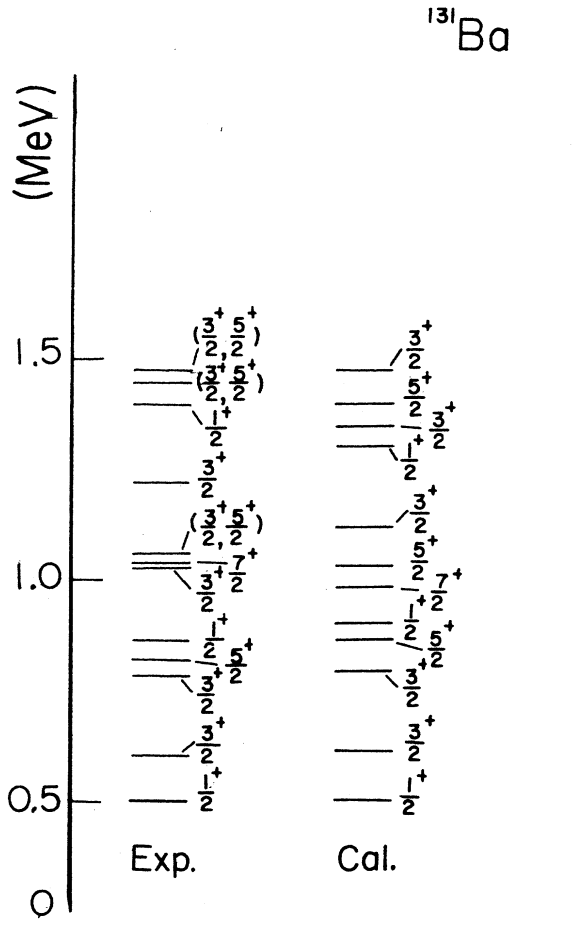

FIG. 8. The calculated and experimental energy spectra for ^{131}Ba. The experimental data are adopted from Ref. 25.

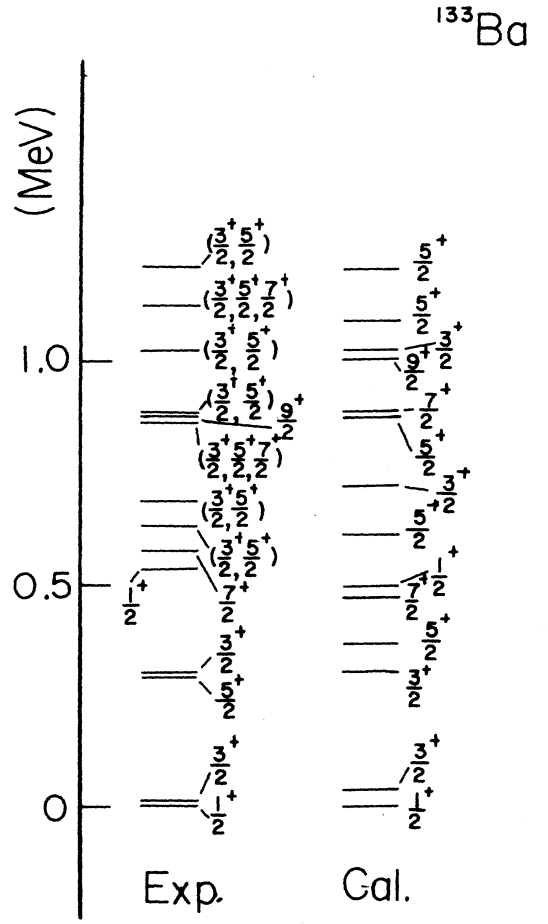

FIG. 9. The calculated and experimental energy spectra for ^{133}Ba. The experimental data are adopted from Ref. 26.

we go to the higher mass end of the isotope string. For example, for ^{129}Xe the lowest $(\frac{1}{2})^+$, $(\frac{3}{2})^+$ states are still the corresponding single-particle states, whereas the lowest $(\frac{5}{2})^+$ and $(\frac{7}{2})^+$ states are mixtures of the configurations of several corresponding single-particle orbits. This is, of course, due to the fact that the $2d_{5/2}$ and $1g_{7/2}$ orbits are already quite high for ^{129}Xe. The band structures are more prominent for the low mass isotopes. For example, the $1g_{7/2}$ quasiband states for ^{123}Xe are clearly dominated by the configurations of the $g_{7/2}$ orbit, while this band disappears for ^{129}Xe. This trend is also consistent with the rising of the $1g_{7/2}$ orbit versus the increase of mass number of the isotopes. The wave functions of the Ba isotopes show similar features as those of the Xe isotopes. Therefore, they are not displayed explicitly.

C. Electromagnetic $E2$ transitions

The $E2$ transition operator in the IBFA-1 model can be written as

$$T^{(2)}=e_B T_B^{(2)}+e_B T_f^{(2)} ,$$

$$T_B^{(2)}=(s^\dagger\times\tilde{d}+d^\dagger\times\tilde{s})^{(2)}+\chi(d^\dagger\times\tilde{d})^{(2)} ,$$

$$T_F^{(2)}=\sum_{ij} T_{ij}^{(2)}(a_i^\dagger\times\tilde{a}_j)^{(2)} ,$$

where $T_{ij}^{(2)}=\langle r^2\rangle\langle i||Y^2||j\rangle/\sqrt{5}$.

In calculating the $E2$ transition rates, the boson and fermion effective charges e_B and e_F were chosen to be 0.13 and -0.15 e, respectively. The minus sign of e_F comes from the holelike nature of the odd neutron. These values are the same as those used in Ref. 9. In the calculation, it was found that the calculated $B(E2)$ values did not depend on the value of e_F sensitively. This is because that the contribution to the transition rates from the boson part is much lager than that from the fermion part.[17] The calculated and experimental $B(E2)$ values for ^{129}Xe and ^{131}Xe are shown in Tables IV and V for comparison. In the tables, the results of Ref. 9 are also displayed for comparison. In general, the calculated values agree with the experimental data reasonably well. Also, the quality of agreement is similar to that obtained in Ref. 9. Since the $B(E2)$ values depend on the wave functions quite sensitively. This suggests that the wave functions obtained in this work are quite reliable.

IV. SUMMARY

The positive parity states of the transitional even-odd Xe, Ba isotopes were studied in IBFA-1. Four fermion single-particle orbits, the $3s_{1/2}$, $2d_{3/2}$, $2d_{5/2}$, and $1g_{7/2}$ orbits were included in the calculation. However, the BCS correlation of the boson-fermion interaction parameter were omitted in the multi-j orbit calculation. In fact, since the boson-boson interaction parameters were fixed by the calculations on the boson core nuclei and the less important boson-fermion monopole interaction was omitted, there are only two free varying boson-fermion interaction parameters for each even-odd nucleus. It was found that the interaction parameters changed quite smoothly versus the change of the mass number of the isotopes. The energy spectra of the Xe isotopes are

TABLE III. The calculated wave function intensities associated with the configurations of each fermion single-particle orbit for ^{123}Xe.

	$(\frac{1}{2})_1^+$	$(\frac{3}{2})_1^+$	$(\frac{3}{2})_2^+$	$(\frac{5}{2})_1^+$	$(\frac{5}{2})_2^+$	$(\frac{7}{2})_1^+$	$(\frac{7}{2})_2^+$	$(\frac{9}{2})_1^+$	$(\frac{11}{2})_1^+$	$(\frac{13}{2})_1^+$	$(\frac{15}{2})_1^+$	$(\frac{17}{2})_1^+$	$(\frac{19}{2})_1^+$
$3s_{1/2}$	0.888	0.081	0.674	0.001	0.645	0.000	0.060	0.000	0.000	0.000	0.000	0.000	0.000
$2d_{3/2}$	0.111	0.861	0.237	0.074	0.296	0.005	0.720	0.008	0.008	0.011	0.008	0.011	0.008
$2d_{5/2}$	0.001	0.057	0.054	0.863	0.047	0.065	0.181	0.116	0.078	0.135	0.077	0.137	0.070
$1g_{7/2}$	0.000	0.001	0.036	0.063	0.012	0.929	0.039	0.876	0.914	0.854	0.915	0.852	0.922

TABLE IV. The calculated and experimental $B(E2)$ values [in $(e\,\mathrm{b})^2$] for ^{129}Xe. The experimental data are adopted from Refs. 18–20.

	Expt.	Ref. 9	This work
$\frac{3}{2}_2 \rightarrow \frac{3}{2}_1$	$<5\times10^{-4}$	0.027	0.037
$\frac{3}{2}_2 \rightarrow \frac{1}{2}_1$	0.12(1)	0.101	0.070
$\frac{5}{2}_1 \rightarrow \frac{3}{2}_1$	0.22(3)	0.085	0.083
$\frac{5}{2}_1 \rightarrow \frac{1}{2}_1$	0.77(7)	0.052	0.110
$\frac{1}{2}_2 \rightarrow \frac{1}{2}_1$	0.044(11)	0.080	0.041
$\frac{5}{2}_2 \rightarrow \frac{1}{2}_1$	0.057(4)	0.067	0.031
$\frac{3}{2}_3 \rightarrow \frac{1}{2}_1$	0.0032(2)	0.011	0.011
$\frac{3}{2}_4 \rightarrow \frac{1}{2}_1$	0.0032(2)	0.001	0.005

TABLE V. The calculated and experimental $B(E2)$ values [in $(e\,\mathrm{b})^2$] for ^{131}Xe. The experimental data are adopted from Refs. 18 and 19.

	Expt.	Ref. 9	This work
$\frac{1}{2}_1 \rightarrow \frac{3}{2}_1$	0.0039(5)	0.009	0.007
$\frac{5}{2}_1 \rightarrow \frac{1}{2}_1$	0.030(5)	0.028	0.032
$\frac{5}{2}_1 \rightarrow \frac{3}{2}_1$	0.10(1)	0.080	0.075
$\frac{3}{2}_2 \rightarrow \frac{3}{2}_1$	0.057(4)	0.065	0.056
$\frac{1}{2}_1 \rightarrow \frac{3}{2}_1$	0.048(4)	0.070	0.024
$\frac{7}{2}_1 \rightarrow \frac{5}{2}_1$	0.005(4)	0.003	0.003
$\frac{7}{2}_1 \rightarrow \frac{3}{2}_1$	0.081(6)	0.092	0.084
$\frac{3}{2}_3 \rightarrow \frac{3}{2}_1$	0.027(2)	0.022	0.020
$\frac{5}{2}_2 \rightarrow \frac{3}{2}_2$	<0.031	0.006	0.005
$\frac{5}{2}_2 \rightarrow \frac{1}{2}_1$	0.068(9)	0.071	0.061
$\frac{5}{2}_2 \rightarrow \frac{3}{2}_1$	0.013(1)	0.019	0.027
$\frac{7}{2}_2 \rightarrow \frac{3}{2}_1$	0.0050(5)	0.0002	0.003

characterized by different quasibands built on the single quasiparticle states. All of these quasibands can be reproduced. The disappearance of the $(\frac{5}{2})^+$ and $(\frac{7}{2})^+$ quasibands for the heavier Xe and Ba isotopes are closely related to the rising of the $(\frac{5}{2})^+$ and $(\frac{7}{2})^+$ quasiparticle energies.

The analyses of the wave functions indicate that the configurations of the wave functions with respect to the fermion orbits become more dispersive as one moves to the heavier isotopes. This tendency is also consistent with the disappearance of some quasibands in the heavier isotopes. The $B(E2)$ values of ^{129,131}Xe can be reproduced reasonably well by the calculated wave functions. This indicates that the wave functions which are not directly produced from the least-squares fits are still quite acceptable.

The energy spectra of the even-even Xe, Ba isotopes in this region do not show very predominant rotational or vibrational characteristics. This may explain the reason why it is difficult to correlate all nuclei in the isotope string by a single geometrical collective model. The IBA model has the advantage of treating all kinds of deformations on an equal footing. The averaged multi-j IBFA model used in this work has the merit of simplicity. The result obtained in this work seems to be quite encouraging. It indicates that the relative importance of each fermion single-particle orbit is mainly determined by its quasiparticle energy. The occupation-number-distribution correlations in the boson-fermion interactions seem to be less important and can be omitted. The model can be used to calculate many other nuclear properties of the even-odd nuclei. For example, the negative parity states of the Xe and Ba isotopes in the same region can be computed by the same model. Also, the model may be applied to other transitional even-odd nuclei. More explorations of the model will shed light on the domain of applicability of the model.

This work is supported by the National Science Council, Republic of China, with Grant No. NSC77-0208-M110-16.

[1] J. Meyer-Ter-Vehn, Nucl. Phys. **A249**, 111 (1975).
[2] J. Gizon, A. Gizon, and J. Meyer-Ter-Vehn, Nucl. Phys. **A277**, 464 (1977).
[3] J. Gizon and A. Gizon, Z. Phys. A **285**, 259 (1978).
[4] K. Heyde and P. J. Brussaard, Nucl. Phys. **A104**, 81 (1967).
[5] K. Heyde and P. J. Brussaard, Z. Phys. **259**, 15 (1973).
[6] F. Donau and S. Frauendorf, Phys. Lett. **71B**, 263 (1977).
[7] F. Iachello and O. Scholten, Phys. Rev. Lett. **43**, 679 (1979).
[8] M. A. Cunningham, Nucl. Phys. **A385**, 204 (1985).
[9] M. A. Cunningham, Nucl. Phys. **A385**, 221 (1985).
[10] J. M. Arias, C. E. Alonso, and R. Bijker, Nucl. Phys. **A445**, 333 (1985).
[11] O. Scholten and A. E. L. Dieperink, in *Interacting Bose-Fermi Systems in Nuclei*, edited by F. Iachello (Plenum, New York, 1981).
[12] F. Iachello and I. Talmi, Rev. Mod. Phys. **59**, 339 (1987).
[13] R. Bijker and A. E. L. Dieperink, Nucl. Phys. **A379**, 221 (1982).
[14] H. Harter, A. Gelberg, and P. Von Brentano, Phys. Lett. **157B**, 1 (1988).
[15] *Table of Isotopes*, 7th ed., edited by C. M. Lederer and V. S. Shirley (Wiley, New York, 1977).
[16] A. Bohr and M. Mottelson, *Nuclear Structure* (Benjamin, New York, 1969), Vol. 1.
[17] N. Yoshida, A. Arima, and T. Otsuka, Phys. Lett. **114B**, 86 (1982).
[18] D. C. Palmer, A. D. Irving, P. D. Forsyth, I. Hall, D. G. E. Martin, and M. J. Maynard, J. Phys. G **4**, 1143 (1978).
[19] A. D. Irving, P. D. Forsyth, I. Hall, and D. G. E. Martin, J. Phys. G **5**, 1595 (1979).
[20] G. Marest, R. Haroutunian, I. Berkes, M. Meyer, M. Rots, J. Deraedt, H. Van de Voode, H. Oonis, and R. Coussement,

Phys. Rev. C **10**, 402 (1974).
[21]A. Lunkko, J. Hattula, H. Helppi, O. Knuuttila, and F. Donau, Nucl. Phys. **A347**, 319 (1981).
[22]H. Helppi, J. Hattula, and A. Lunkko, Nucl. Phys. **A332**, 183 (1979).
[23]H. Helpppi, J. Hattula, A. Lunkko, M. Jaaskelainen, and F. Donau, Nucl. Phys. **A357**, 333 (1981).
[24]P. Brodeur, B. P. Pathak, and S. K. Mark, Z. Phys. A **289**, 289 (1979).
[25]R. L. Auble, H. R. Hiddelston, and C. P. Browne, Nucl. Data Sheets **17**, 573 (1976).
[26]Yu V. Sergeenkov and V. M. Sigalov, Nucl. Data Sheets **49**, 660 (1986).